

1 Article

2 

# Transforming Growth Factor- $\beta$ 3 Chitosan Sponge (TGF- 3 $\beta$ 3/CS) Facilitates Osteogenic Differentiation of 4 Human Periodontal Ligament Stem Cells

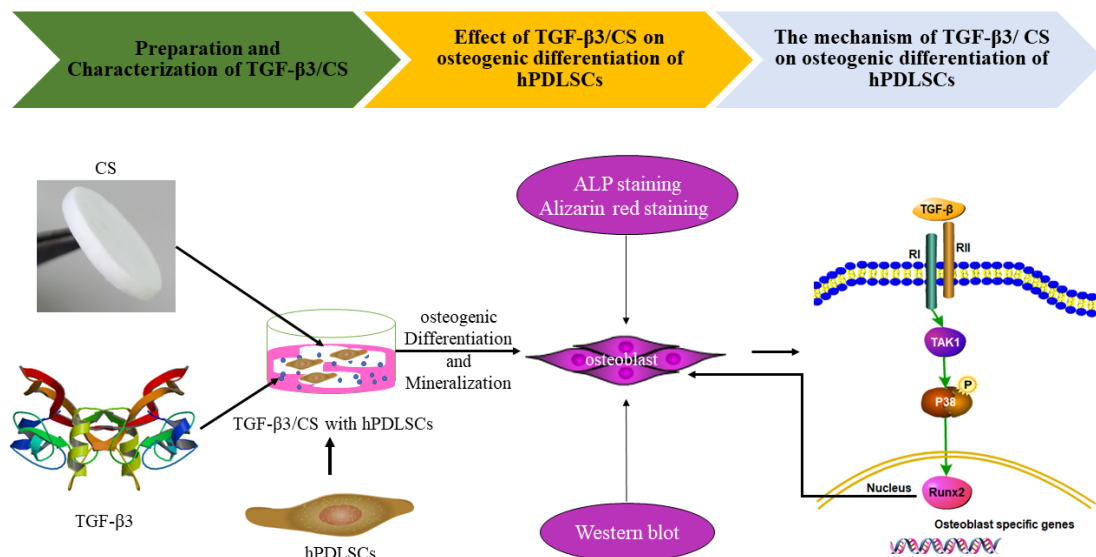
5 **Yangfan Li** <sup>1,†</sup>, **Zhifen Qiao** <sup>1,†</sup>, **Fenglin Yu** <sup>1</sup>, **Huiting Hu** <sup>2</sup>, **Yadong Huang** <sup>1</sup>, **Qi Xiang** <sup>1,\*</sup>, **Qihao**  
6 **Zhang** <sup>1</sup>, **Yan Yang** <sup>1</sup> and **Yueping Zhao** <sup>2</sup>7 <sup>1</sup> Institute of Biomedicine and Guangdong Provincial Key Laboratory of Bioengineering Medicine, Jinan  
8 University, Guangzhou 510632, PR China9 <sup>2</sup> Department of Stomatology, Jinan University Medical College, Guangzhou 510632, China10 <sup>†</sup> Yangfan Li and Zhifen Qiao contributed equally to this work.11 <sup>\*</sup> Correspondence: Qi Xiang, Institute of Biomedicine and Guangdong Provincial Key Laboratory of  
12 Bioengineering Medicine, Jinan University, Guangzhou 510632, PR China, E-mail address:  
13 txiangqi@jnu.edu.cn (Q Xiang).

14

15 **Abstract:** Periodontal disease is the main reason for tooth loss in adults. Tissue engineering and  
16 regenerative medicine are the advanced technologies used to manage soft and hard tissue defects  
17 caused by periodontal disease. We developed a transforming growth factor- $\beta$ 3 chitosan sponge  
18 (TGF- $\beta$ 3/CS) to repair periodontal soft and hard tissue defects. We investigated the proliferation  
19 and osteogenic differentiation behaviors of primary human periodontal ligament stem cells  
20 (hPDLSCs) to discuss the bioactivity and application of TGF- $\beta$ 3 in periodontal disease. We  
21 separately used Calcein-AM/PI double-labeling or CM-Dil-labeling coupled with fluorescence  
22 microscopy to trace the survival and function of the cells after implantation in vitro or in vivo. The  
23 mineralization of osteogenic differentiated hPDLSCs was confirmed by measuring ALP activity and  
24 calcium content. The levels of COL I, ALPL, TGF- $\beta$ RI, TGF- $\beta$ RII, and Pp38/t-p38 were tested using  
25 Western blot to explore the mechanism of bone repair prompted by TGF- $\beta$ 3. When hPDLSCs were  
26 inoculated with different concentrations of TGF- $\beta$ 3/CS (62.5–500 ng/mL), ALP activity was the  
27 highest in TGF- $\beta$ 3 (250 ng/mL) group after seven days ( $P < 0.05$  vs. control); the calcium content in  
28 each group increased significantly after 21 and 28 days ( $P < 0.001$  vs. control). The best result was  
29 achieved in the TGF- $\beta$ 3 (500 ng/mL) group. All results showed that TGF- $\beta$ 3/CS can promote  
30 osteogenic differentiation of hPDLSC and may be involved in the p38 MAPK signaling pathway.  
31 TGF- $\beta$ 3/CS has the potential for application in the repair of incomplete alveolar bone defects.32 **Keywords:** transforming growth factor  $\beta$ 3; chitosan sponge; human periodontal ligament cells;  
33 osteogenic differentiation

34

35 **Graphical Abstract**



36

37 **1. Introduction**

38 Periodontal disease is a chronic inflammatory condition that affects the supporting tissues  
 39 around the teeth, resulting in periodontal tissue breakdown or tooth loss in severe cases. Being highly  
 40 prevalent among adults, periodontal disease treatment is receiving increased attention from  
 41 researchers and clinicians [1]. Therefore, repairing periodontal support tissues such as alveolar bone  
 42 is an indispensable part of the treatment of periodontal disease. With the increasing popularity of  
 43 dental implant surgery, the lack of bone mass in patients with periodontitis has limited the need for  
 44 implant surgery, and the need for repair of alveolar bone defects is increasing [2,3].

45 The current clinical techniques mainly used for the treatment of alveolar bone defects [4] are  
 46 bone grafting and guided bone regeneration (GBR). Autologous bone grafting is considered to be the  
 47 gold standard of bone repair [5-8], but it has many limitations, such as longer operation and recovery  
 48 times, patients with insufficient bone mass, and a number of complications are possible [9,10]. GBR  
 49 uses a barrier to provide space and is filled with new bone to compensate for these deficiencies [11,12].  
 50 However, GBR has shortcomings such as immune rejection, and poor morphological structure and  
 51 mechanical properties [13-15]. In recent years, periodontal tissue engineering technology,  
 52 characterized by the use of (stem) cells, bioactive molecules (e.g., growth factors), and scaffold  
 53 materials as the three basic elements, has provided a new solution for reconstructing alveolar bone  
 54 defects.

55 Transforming growth factor- $\beta$ 3 (TGF- $\beta$ 3) has been used for cartilage repair, tissue regeneration  
 56 and wound healing *in vivo* [16-18]. TGF- $\beta$ 3 facilitates matrix formation, immunity, as well as  
 57 maintenance of stem cell characteristics [19]. TGF- $\beta$ 3 promotes the proliferation and early  
 58 differentiation of mesenchymal stem cells (MSCs) into osteoblasts, chondrocytes, adipocytes and  
 59 tendon cells [20]. TGF- $\beta$ 3 can also recruit endogenous mesenchymal stem cells to initiate bone  
 60 regeneration [21-24]. TGF- $\beta$ 3 can induce endochondral bone formation [25] and complete bone  
 61 remodeling [26]. It may play a profound role in some osteogenic stages, so TGF- $\beta$ 3 can be considered  
 62 a selective bioactive molecule for repairing alveolar bone defects. Moioli et al. [27] demonstrated for  
 63 the first time that autologous MSCs and controlled-release TGF- $\beta$ 3 can reduce the surgical trauma  
 64 due to local osteotomy. However, TGF- $\beta$ 3 is easily degrades, inactivates, and spreads. Therefore, it  
 65 was necessary to develop some carrier materials to carry it. Chitosan is a natural polymer material  
 66 that can effectively promote wound healing and early osteogenesis after tooth extraction [28]. It  
 67 would be an ideal carrier of TGF- $\beta$ 3.

68 Alveolar bone regeneration is enhanced by the addition of osteogenic cells to biomaterial  
 69 scaffolds, which can reduce treatment time and produce better outcomes and increase patient comfort  
 70 [29]. Periodontal ligament stem cells (PDLSCs) promote osteoblastic and osteoclastic differentiation

71 of osteoblast, and form an ectopic cementum/ligament-like complex [30]. Kim et al. [31] reported that  
72 the growth and induction of PDLSCs promote the regeneration of cementum and periodontal  
73 ligament, to enable easy root fixation and resorption. As PDLSC is one the suitable stem cells for  
74 periodontal tissue regeneration, we employed hPDLSCs to validate TGF- $\beta$ 3 in regeneration of  
75 alveolar bone defects.

76 By comparison of our results with those reported previously, we found that PDLSCs undergo  
77 osteogenic differentiation through the mitogen-activated protein kinase (MAPK) signaling pathway  
78 [32-34], and that signaling transduction mediated by TGF- $\beta$ 3 in osteogenic differentiation and bone  
79 regeneration [35] specifically occurs through both canonical Smad-dependent pathways (TGF- $\beta$   
80 ligands, receptors, and Smads) and non-canonical Smad-independent signaling pathway (e.g., p38  
81 MAPK pathway). We hypothesized that TGF- $\beta$ 3 may promote osteogenic differentiation of hPDLSCs  
82 via the p38 MAPK pathway. So, we tested the levels of COL I, ALPL, TGF- $\beta$ RI, TGF- $\beta$ RII, and  
83 Pp38/p38 by Western blot.

84 TGF- $\beta$ 3/CS facilitated the osteogenic differentiation of hPDLSCs in this study. We further  
85 examined and verified the mechanism through which TGF- $\beta$ 3 promotes osteogenic differentiation of  
86 hPDLSCs. TGF- $\beta$ 3 may be combined with hPDLSCs for the regeneration of alveolar bone defects.

## 87 2. Results

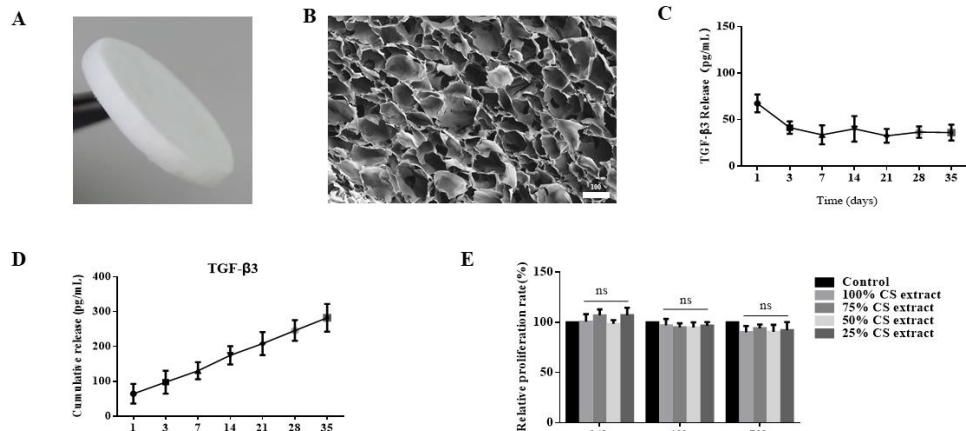
### 88 2.1. Preparation and Characterization of TGF- $\beta$ 3/CS

89 As shown in Figure 1A, CS has a regular appearance and a smooth surface. In the SEM image,  
90 TGF- $\beta$ 3/CS showed a three-dimensional (3D) porous network structure, and interpenetrating pore  
91 structures resulted in a large internal surface area (Figure 1B). The pore size of the TGF- $\beta$ 3/CS was  
92  $156.95 \pm 18.21 \mu\text{m}$ , the water absorption was  $2347\% \pm 201\%$ , the swelling ratio was  $52.67\% \pm 12.42\%$ ,  
93 and the porosity was  $85.65\% \pm 3.5\%$ .

94 As shown in Figure 1C, TGF- $\beta$ 3 can be stably released from CS at predetermined time points,  
95 cumulatively released in CS, and continues to act on the cells (Figure 1D). The biocompatibility of the  
96 TGF- $\beta$ 3/CS was evaluated using the MTT assay. Compared with the control group, the scaffold had  
97 no obvious cytotoxicity ( $P > 0.05$ ; Figure 1E). Therefore, CS is a suitable carrier of TGF- $\beta$ 3, ensuring  
98 sustained and stable release of TGF- $\beta$ 3 in vivo and in vitro.

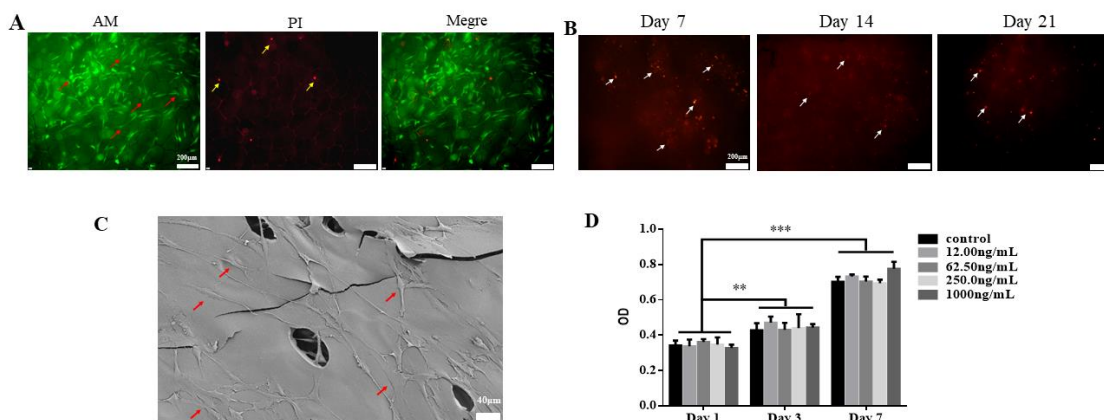
99 After hPDLSCs were cultured on TGF- $\beta$ 3/CS for three days, hPDLSCs grew well. The cell  
100 structure was intact, and there were more viable cells (Figure 2A, green) than dead cells (Figure 2A,  
101 red). TGF- $\beta$ 3/CS with hPDLSCs pre-stained with CM-Dil were implanted subcutaneously into SD  
102 rats for 7, 14, and 21 days to observe the growth of cells (Figure 2B). The red viable cells were also  
103 observed after 21 days, indicating that TGF- $\beta$ 3/CS with hPDLSCs can survive well in animals.

104 After hPDLSCs were seeded in TGF- $\beta$ 3/CS for seven days, hPDLSCs displayed good adhesion  
105 and extension state on the surface of CS, and the cells adhered to each other to form a sheet growth,  
106 and some cells crossed the pores of the porous sponge (Figure 2C). After inoculation of hPDLSCs on  
107 CS with different concentrations of TGF- $\beta$ 3, we observed that hPDLSCs could grow and proliferate  
108 on CS ( $P < 0.001$  vs. control; Figure 2D).



109

110 **Figure 1.** Characterization of TGF- $\beta$ 3/CS and Release of TGF- $\beta$ 3 from CS. (A). CS photographs. (B).  
 111 The scanning electron microscope (SEM) CS image. Scale bar represents 100  $\mu$ m. (C). The release curve  
 112 of TGF- $\beta$ 3 from CS (mean  $\pm$  SD;  $n$  = 3). (D). The cumulative release of TGF- $\beta$ 3 from CS (mean  $\pm$  SD;  $n$   
 113 = 3). (E). Cytotoxicity assay of CS extract measured by MTT assay (mean  $\pm$  SD;  $n$  = 5). Blank control  
 114 group: cells were cultured only with the extraction medium; CS extract group: cells were cultured  
 115 with 25%, 50%, 75%, or 100% CS extract.



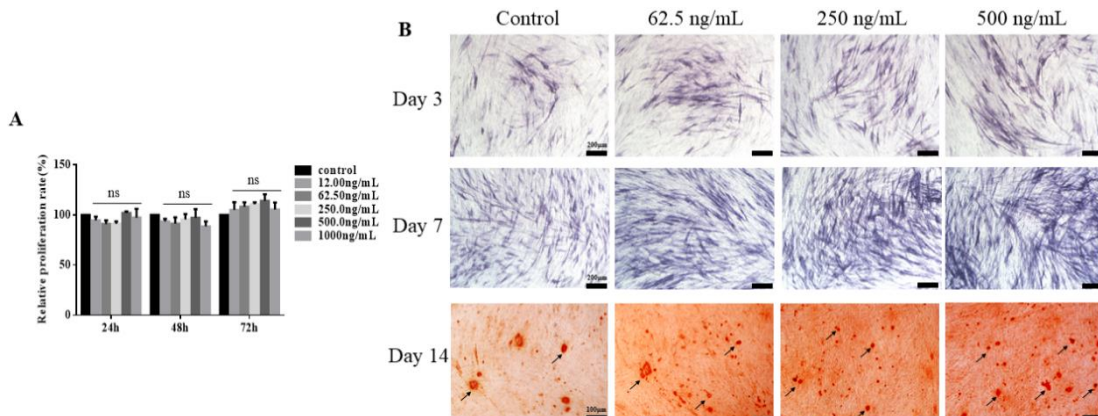
116

117 **Figure 2.** Effect of TGF- $\beta$ 3/CS on the growth and proliferation of hPDLSCs. (A) Calcein-AM staining  
 118 of hPDLSCs on TGF- $\beta$ 3/CS after three days of culture; live cells (red arrow) are stained by AM (green),  
 119 and dead cells (yellow arrow) are stained by PI (red). Scale bar represents 200  $\mu$ m. (B) TGF- $\beta$ 3/CS  
 120 with hPDLSCs (white arrow) implant Sprague-Dawley rats for 7, 14, and 21 days, and then stained  
 121 with CM-Dil (red). The cell survival was observed using a fluorescence microscope. (C) SEM  
 122 photomicrographs of hPDLSCs (red arrow) in CS for seven days. Scale bar represents 40  $\mu$ m. (D)  
 123 hPDLSCs growth in TGF- $\beta$ 3/CS was measured by CCK-8 (mean  $\pm$  SD;  $n$  = 5). \*P < 0.05 vs. control; \* \*  
 124 P < 0.01 vs. control; \*\*\*P < 0.001 vs. control.

125 **2.2. TGF- $\beta$ 3 Does Not Affect Growth and Proliferation of hPDLSCs but Facilitates Its Osteogenic  
 126 Differentiation**

127 The relative proliferation rate of hPDLSCs cultured at different concentrations of TGF- $\beta$ 3 for 24,  
 128 48, and 72 h was examined using the MTT assay. The relative proliferation rates depended on time,  
 129 but they did not change with the concentration of TGF- $\beta$ 3. TGF- $\beta$ 3 did not significantly promote or  
 130 inhibit the growth or proliferation of hPDLSCs within the concentration gradient range ( $P > 0.05$ , vs.  
 131 control), and the high concentration showed no significant toxicity to hPDLSCs (Figure 3A). However,  
 132 as shown in Figure 3B, TGF- $\beta$ 3 promoted ALP secretion and calcium deposition of hPDLSCs. When  
 133 the loading of TGF- $\beta$ 3 was 250 or 500 ng/mL, the expressions of ALP and calcium in hPDLSCs were

134 significantly up-regulated. The optimal concentration range of TGF- $\beta$ 3 in promoting cell  
135 differentiation is 250–500 ng/mL.



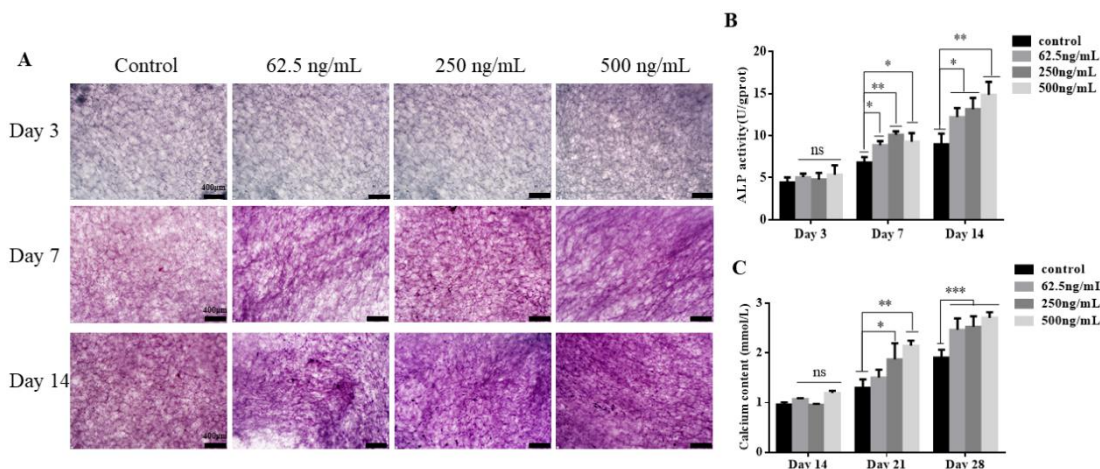
136  
137  
138  
139  
140  
141  
142  
143

**Figure 3.** TGF- $\beta$ 3 does not affect the growth and proliferation of hPDLSCs, but can promote its osteogenic differentiation. (A). The relative proliferation rate of hPDLSCs cultured at different concentrations of TGF- $\beta$ 3 for 24 h, 48 h and 72 h by MTT assay (n=5). (B). Alkaline phosphatase (ALP) staining (purple) was used to detect the ALP activity of hPDLSCs with different concentrations of TGF- $\beta$ 3 after 3 days and 7 days of osteogenic induction; Alizarin red staining (red) was used to detect the calcium content of hPDLSCs with different concentrations of TGF- $\beta$ 3 after 14 days of osteogenic induction. Black arrow shows calcium deposition.

#### 144 2.3. TGF- $\beta$ 3/CS Facilitates Osteogenic Differentiation of hPDLSCs

145 hPDLSCs were inoculated on CS with different concentrations of TGF- $\beta$ 3 (62.5, 250, and 500  
146 ng/mL), and ALP values were determined for 3, 7, and 14 days after osteoblastic induction (Figure  
147 4A). We observed no significant difference in any TGF- $\beta$ 3/CS group compared with CS for three days,  
148 but TGF- $\beta$ 3/CS groups exhibited significant differences after 7 and 14 days (P < 0.05, vs. control;  
149 Figure 4B).

150 The calcium content was measured after osteogenic induction for 14, 21, and 28 days. No  
151 significant differences we observed in any groups for 14 days, but every TGF- $\beta$ 3/CS group had  
152 significantly higher levels of calcium content for 21 and 28 days (P < 0.05, vs. control). The best results  
153 were recorded for the TGF- $\beta$ 3 (500 ng/mL)/CS group (P < 0.001, vs. control) (Figure 4C).



154  
155  
156  
157  
158

**Figure 4.** Effect of TGF- $\beta$ 3/CS on osteogenic differentiation of hPDLSCs. (A). ALP staining (purple) was used to detect the ALP activity of hPDLSCs on CS with different concentrations of TGF- $\beta$ 3 after 3 days, 7 days and 14 days of osteogenic induction. (B). Detection of ALP activity of hPDLSCs on CS with different concentrations of TGF- $\beta$ 3 after 3 days, 7 days and 14 days of osteogenic induction. (C).

159 Determination of calcium of hPDLSCs on CS with different concentrations of TGF- $\beta$ 3 after 14d, 21d  
 160 and 28d of osteogenic induction(n=3). \*  $P < 0.05$  vs. control; \*\*  $P < 0.01$  vs. control.; \*\*\*  $P < 0.001$  vs.  
 161 control.

162 **2.4. TGF- $\beta$ 3 Promotes Osteogenic Differentiation of hPDLSCs via p38 MAPK Pathway**

163 To verify the effect of TGF- $\beta$ 3 on osteogenic differentiation of hPDLSCs, we examined the  
 164 changes in osteogenic-associated proteins (COL I, COL II, and ALPL) and pathway proteins (TGF-  
 165  $\beta$ RI, TGF- $\beta$ RII, p38, Pp38, and Runx2) with induction time and TGF- $\beta$ 3 concentration via Western blot  
 166 (Figures 5A and 6B). There was a statistically significant difference in the increase in COLI expression  
 167 in the TGF- $\beta$ 3 (500 ng/mL) induction group after 7 and 14 days' induction ( $P < 0.001$ , vs. control),  
 168 whereas the other induction groups showed no statistical differences ( $P > 0.05$ , vs. control). The  
 169 amount of COLI expression induced after 14 days was significantly higher than that after 7 days  
 170 (Figure 5B).

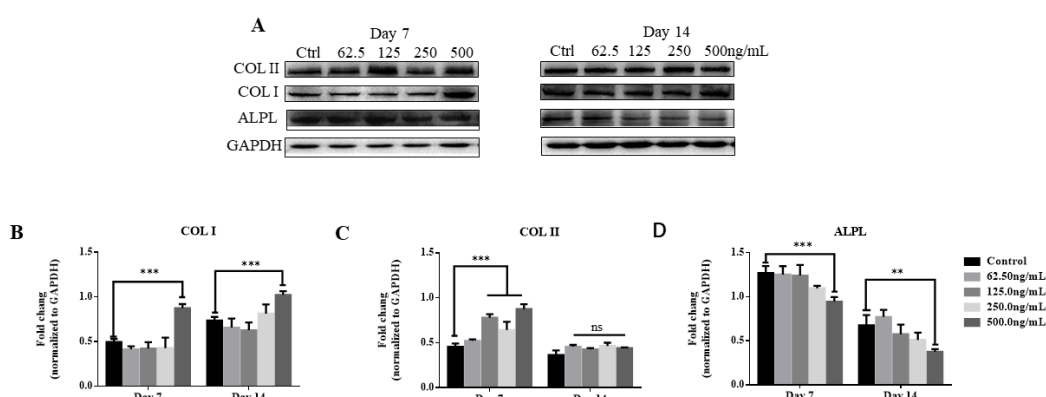
171 The expression of COL II significantly increased in TGF- $\beta$ 3 (125, 250, and 500 ng/mL) induction  
 172 groups after seven days' induction ( $P < 0.001$ , vs. control); after 14 days, there was no statistical  
 173 difference in the induction groups ( $P > 0.05$ , vs. control). Compared with the day 7 results, TGF- $\beta$ 3  
 174 (125, 250, and 500 ng/mL) induction groups for day 14 were significantly reduced (Figure 5C).

175 The expression of ALPL was significantly decreased in the TGF- $\beta$ 3 (500 ng/mL) induction  
 176 groups after 7 and 14 days of induction ( $P < 0.01$ , vs. control), and no significant difference was found  
 177 in the other groups ( $P > 0.05$ , vs. control). The ALPL expression induced for 14 days was significantly  
 178 lower than that for 7 days (Figure 5D).

179 In conclusion, as the induction time increased, the COL I of the TGF- $\beta$ 3 (500 ng/mL) induction  
 180 group increased significantly, and the COL II and ALPL decreased significantly.

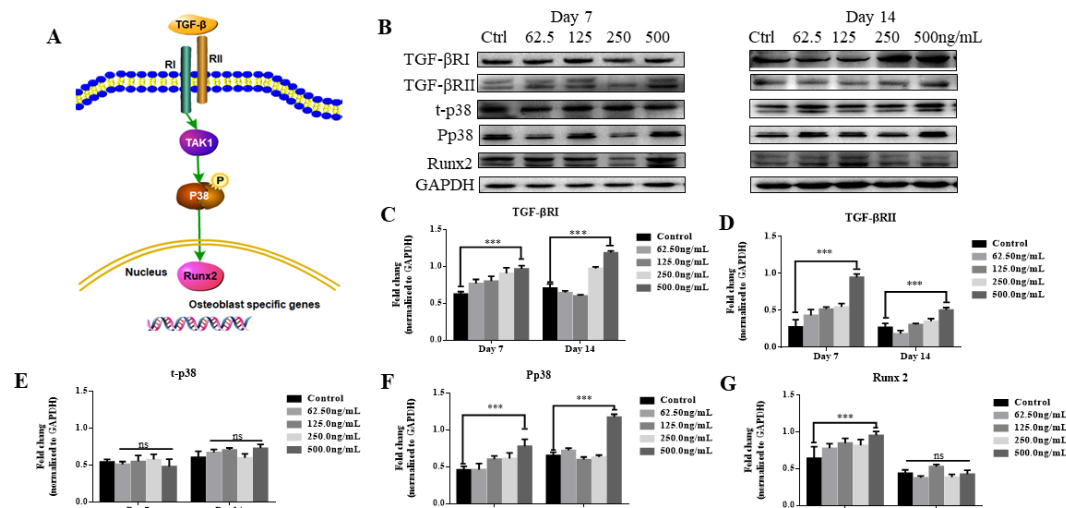
181 The expression of TGF- $\beta$ RI was significantly increased in TGF- $\beta$ 3 (500 ng/mL) induction groups  
 182 after 7 and 14 days' induction ( $P < 0.001$ , vs. control). The expression of TGF- $\beta$ RI induced for 14 days  
 183 was significantly higher than for 7 days (Figure 6C). The expression of TGF- $\beta$ RII in the TGF- $\beta$ 3 (500  
 184 ng/mL) induction group was significantly increased after 7 and 14 days' induction. ( $P < 0.001$ , vs.  
 185 control). The TGF- $\beta$ RII expression induced for 14 days was significantly lower than for 7 days (Figure  
 186 6D). No significant difference was found in the expression of t-p38 in the induction group after 7 and  
 187 14 days' induction ( $P > 0.05$ , vs. control) (Figure 6E), whereas the expression of Pp38 was significantly  
 188 increased in the TGF- $\beta$ 3 (500 ng/mL) induction group ( $P < 0.001$ , vs. control). The Pp38 induced for  
 189 14 days was significantly higher than for 7 days (Figure 6F). The expression of Runx2 in the TGF- $\beta$ 3  
 190 (500 ng/mL) induction group was significantly increased after seven days of induction ( $P < 0.001$ , vs.  
 191 control); after 14 days, no statistical difference was found in the induction group ( $P > 0.05$ , vs. control).  
 192 The expression of Runx2 induced for 14 days was significantly lower than for 7 days (Figure 6G).

193 In conclusion, as the induction time increased, TGF- $\beta$ RI and Pp38 in the TGF- $\beta$ 3 (500 ng/mL)  
 194 induction group increased significantly, the TGF- $\beta$ RII and Runx2 decreased significantly, and t-p38  
 195 was unchanged (Figure 6C). So, Pp38/t-p38 showed an up-regulated trend, indicating that TGF- $\beta$ 3  
 196 can significantly increase osteogenic differentiation of hPDLSCs.



198  
199  
200  
201  
202  
203

**Figure 5.** Expression and analysis of proteins associated with osteogenic differentiation. (A-D) After osteogenic induction of hPDLSCs with different concentrations of TGF- $\beta$ 3 for 7 and 14 days, the expression of osteogenic proteins (COL I, COL II, and ALPL) were detected by (A) Western blot and analyzed by gray scale scanning for (B) COL I, (C) COL II and (D) ALPL (n = 3). \* P < 0.05 vs. control; \*\* P < 0.01 vs. control.; \*\*\* P < 0.001 vs. control. Abbreviations: Col I, type I collagen; Col II, type II collagen; ALPL, Alkaline phosphatase.

204  
205  
206  
207  
208  
209  
210  
211  
212

**Figure 6.** The mechanism of TGF- $\beta$ 3 on osteogenic differentiation of hPDLSCs based on this study. (A) Schematic representation of the mechanism of TGF- $\beta$ 3 on osteogenic differentiation of hPDLSCs. (B) After osteogenic induction of hPDLSCs with different concentrations of TGF- $\beta$ 3 for 7 and 14 days, the expression of osteogenic pathway proteins were detected by (B) Western blot and analyzed by gray scale scanning for (C) TGF- $\beta$ RI, (D) TGF- $\beta$ RII, (E) t-p38, (F) Pp38 and (G) Runx2 (n=3). \* P < 0.05 vs. control; \*\* P < 0.01 vs. control; \*\*\* P < 0.001 vs. control. Abbreviations: TGF- $\beta$ RI, transforming growth factor- $\beta$  receptor I; TGF- $\beta$ RII, transforming growth factor- $\beta$  receptor II; t-p38, total p38; Pp38, phosphorylated p38; Runx2, runtrelated transcription factor 2.

213

### 3. Discussion

214  
215  
216

The aim of periodontal tissue engineering is to regenerate the tooth's supporting tissue through a combination of proper biomaterials, such as growth factors and scaffold materials, which stimulate cells and signaling molecules to produce new healthy tissue.

217  
218  
219  
220  
221  
222  
223  
224  
225  
226

PDLSCs have broad application prospects as odontogenic seed cells in periodontal tissue engineering and regenerative medicine due to their biosafety and odontogenic properties. Biomaterials that repair alveolar bone defects require stable biological properties and good biocompatibility. Many studies had examined the use of TGF- $\beta$ 3 for cartilage repair, tissue regeneration, and wound healing *in vivo* [36]. In this study, we prepared TGF- $\beta$ 3/CS freeze-dried sponge, which is a high-porosity network material with good water absorption and swelling rate. It can mimic the natural extracellular microenvironment of dental tissue and promote the adhesion, proliferation, and differentiation of hPDLSCs. The morphology and Calcein-AM/PI double staining results showed that hPDLSCs can be spread into a typical fusiform shape on TGF- $\beta$ 3/CS, and continue growing and reproducing.

227  
228  
229  
230  
231

In vitro experiments revealed that TGF- $\beta$ 3/CS does not significantly promote or inhibit the growth and proliferation of hPDLSCs, but promotes osteogenic differentiation of hPDLSCs. *In vivo* experiments verified that hPDLSCs on TGF- $\beta$ 3/CS can survive in animals for a long time. This means TGF- $\beta$ 3/CS has stable biological properties and good biocompatibility, indicating its promise as a biomedical material for future tissue engineering.

232  
233  
234

Osteogenic differentiation of cells is a complex process involving cell proliferation, extracellular matrix maturation, and mineralization [37]. ALP is an enzyme on the cell membrane that can catalyze the hydrolysis of phosphate esters. Its activity can reflect the osteogenic activity and function of cells,

235 and it has the highest expression during the maturity of the extracellular matrix. Therefore, ALP is  
236 one of the important indicators for evaluating the degree of early osteogenic differentiation of cells.  
237 According to the results of ALP staining and its quantitative detection, ALP activity in the TGF- $\beta$ 3  
238 (250 ng/mL)/CS induction group on the seventh day was significantly higher than in the other groups.  
239 Compared with day 7, ALP activity increased at day 14, which is not consistent with the results of ALPL  
240 expression measured by Western blot. This may be due to ALP being a marker of early osteogenic  
241 differentiation of cells, and when cells begin to enter the late stage of osteogenic differentiation, the  
242 ALP secreted by the cells may be accumulated in the supernatant, resulting in an increase in ALP  
243 content. Alizarin red staining is a common method for identifying advanced osteogenic  
244 differentiation of cells [32]. hPDLSCs were cultivated in osteogenic differentiation medium and  
245 stained with alizarin red after cultivation for 14 days, showing that TGF- $\beta$ 3 promotes osteogenic  
246 differentiation. However, hPDLSCs on TGF- $\beta$ 3/CS cannot be stained with alizarin red to detect  
247 calcium ion content, since the high-porosity chitosan material has an adsorption effect on the alizarin  
248 red dyeing solution, so the interference of the material itself cannot be ruled out after the dyeing.  
249 Therefore, we detected and quantified the osteocalcin of hPDLSC in the materials using calcium colorimetry,  
250 which indicated that TGF- $\beta$ 3/CS can increase the expression level of calcium in cells. The TGF- $\beta$ 3  
251 (500ng/mL)/CS group had the highest calcium content, demonstrating that a high concentration of TGF- $\beta$ 3 is  
252 more favorable for osteogenic differentiation of hPDLSCs in the late stage of differentiation.

253 The methods of repairing bone defects can be divided into intramembranous osteogenesis and  
254 endochondral ossification. The former induces osteoblasts to secrete a bone-like matrix  
255 mineralization, whereas the latter induces cartilage cells to produce cartilage matrix and then  
256 gradually mineralize to form bone-like matrix. This experiment was conducted to explore the  
257 mechanism through which TGF- $\beta$ 3 induces osteogenic differentiation. The representative proteins of  
258 osteogenic (COLI and ALPL) and cartilage (COLII) were selected for Western blot detection. COLI  
259 plays an indispensable role in extracellular matrix maturation and formation of mineralized nodules,  
260 and is one of the markers of early osteogenic differentiation of cells [38]. COLII is a major component  
261 of hyaline cartilage and plays a key role in maintaining chondrocyte function; COLII is one of the  
262 important indicators of chondrogenic differentiation. TGF- $\beta$ 3 contributes to the significant  
263 improvement in the formation of type II collagen, inducing and promoting cartilage differentiation  
264 [39]. According to the Western blot results, the expression of COLI in each group was up-regulated with the  
265 prolongation of culture time, and the expression level of COLI in the TGF- $\beta$ 3 (500ng/mL)-induced group was  
266 higher than in the control group. The expression of COLII began to increase gradually and the expression of COLII  
267 in the seven-day TGF- $\beta$ 3-induced group was significantly higher than in the COLI group. This may be due to  
268 TGF- $\beta$ 3 promoting cell differentiation into cartilage in the early stage of cell differentiation. However, the  
269 expression levels of COLII were down-regulated in all induction groups, whereas the expression levels of COLI  
270 were up-regulated. This may be due to the initiation of endochondral ossification in the TGF- $\beta$ 3-induced group  
271 and the entry into the mineralization phase of the cells. Endochondral ossification [40] refers to the process of  
272 depositing collagen and non-collagen on the cartilage to mineralize. Here, the cartilage proliferates, matures, and  
273 hypertrophies, and then the hypertrophic cartilage matrix is gradually replaced by trabecular bone. A decrease in  
274 the expression level of COLII was reported to indicate a stage in which endochondral ossification enters the  
275 cartilage matrix calcification [41]. Another study [42] found that TGF- $\beta$ 3 can induce the ossification of human  
276 adipose stromal cells into bone tissue in the rat bone defect model, and the trend in COLI and COLII protein  
277 expression is basically consistent with the results of this experiment.

278 Studies have shown that bioactive molecules promote the proliferation, migration, and  
279 osteogenic differentiation of PDLSCs by activating the MAPK pathway in vitro [32-34]. Through  
280 contrastive analysis of the mechanism of osteogenic differentiation of TGF- $\beta$ 3 and hPDLSCs, we  
281 hypothesize that TGF- $\beta$ 3 may act through binding TGF- $\beta$ RI/II to first start downstream molecule p38  
282 phosphorylation. Following TGF- $\beta$ 3 induction, the p38 MAPK pathways converge at Runx2 to  
283 control hPDLSCs differentiation. However, Runx2 is the earliest and continuously expressed protein in the  
284 process of cell osteogenesis, marking the beginning of osteogenic differentiation. As shown by the Western blot  
285 results, the day 14 expression was significantly lower than on day 7. This trend is consistent with the results  
286 reported by Paoletta et al. [43]. Other studies [44] have shown that Runx2 plays an important role in coordinating

287 multiple signals involved in osteoblast differentiation and is a specific transcriptional regulator necessary for  
288 osteoblast differentiation and bone formation. The existence of the p38 MAPK pathway was verified by  
289 the Western blot results, but the associated protein TAK1 was not detected, potentially because other  
290 pathways can bypass this protein, enter the downstream, and finally result in osteogenesis, but this  
291 remains to be further verified.

292 **4. Materials and Methods**

293 *4.1. Preparation and Characterization of TGF- $\beta$ 3/CS*

294 CS (molecular weight,  $3.6 \times 10^3$  Da; deacetylation degree, 50%) was purchased from Zhengzhou  
295 Kerui Fine Chemical Co., Ltd (Zhengzhou, China). TGF- $\beta$ 3 was supplied by the Biopharmaceutical  
296 R&D Center of Jinan University (Guangzhou, China). All other chemical reagents obtained from  
297 Shanghai Lingfeng were of analytical grade. Briefly, after CS (1% *w/v*) was lyophilized, we placed it  
298 in a 95% ethanol solution for 2 h and then discarded the ethanol. Next, it was immersed and cleaned  
299 in 10% sodium hydroxide solution for 2 h, then repeatedly cleaned with deionized water until the  
300 pH was about 7. We produced a lyophilized sponge-like biomaterial that was sterilized and stored  
301 for later use. TGF- $\beta$ 3 at different concentrations (0, 62.5, 250, and 500 ng/mL) were loaded on CS by  
302 drop.

303 The water absorption rate, the swelling ratio, and the porosity of CS were calculated as  
304 previously reported [45]. The micromorphology of the prepared CS was observed by scanning  
305 electron microscopy (SEM, XL30; Philips, Amsterdam, Netherlands).

306 *4.1.1. Release Profile of TGF- $\beta$ 3 from CS*

307 The release of TGF- $\beta$ 3 from CS was measured with ELISA (CUSABIO, Wuhan, China). The  
308 scaffold (3 replicates/group) was placed in a 1.5 mL Eppendorf tube, 1 mL MEM was added, which  
309 was incubated at 37 °C for 35 days. We collected 1 mL of MEM supernatant and 1 mL fresh MEM was  
310 added at day 1, 3, 7, 14, 21, 28, and 35. The supernatant samples were maintained at -80 °C until use  
311 for ELISA measurements. ELISA was performed according to the manufacturer's protocol. Light  
312 absorbance was read with a microreader at a wavelength of 450 nm (Thermo Lab systems, Waltham,  
313 MA, USA).

314 *4.2. Culture of hPDLSCs*

315 The hPDLSCs were obtained from tissues attached to the middle third of the tooth root from  
316 healthy 15–20 year old patients (5 men and 5 women) as described previously, who were undergoing  
317 orthodontic treatment at the First Affiliated Hospital of Jinan University [46]. All the experimental  
318 protocols used were approved by the Ethics Committee of Jinan University (Guangdong, China). The  
319 tissues were cut, digested, and cultured with medium supplemented with  $\alpha$ -MEM (Gibco, New York,  
320 USA), 10% fetal bovine serum (FBS, Gibco, New York, USA), 100 mg/mL streptomycin, and 100U/mL  
321 penicillin (MDBio, Shanghai, China) at 37°C in an atmosphere containing 5% CO<sub>2</sub>. The medium was  
322 changed every 3 days and hPDLSCs at passages (P) 3–5 were used in the following experiments.

323 *4.3. Bioactivity and Biocompatibility Assay*

324 *4.3.1. MTT Assay to Test Biocompatibility In Vitro*

325 The cytotoxicity of the CS was evaluated using an extraction test. The ratio between the sample  
326 surface and the volume of the medium was 0.5 cm<sup>2</sup>/mL. In brief, the 3T3 cells (provided by China  
327 National Institute for the Control of Pharmaceutical and Biological Products, Beijing, China) were  
328 cultured in a 96-well plate at a density of  $1 \times 10^4$  cells/well in DMEM and 10% FBS for 24 h. The cells  
329 were then divided into five groups and separately treated with 25% CS extract, 50% CS extract, 75%  
330 CS extract, 100% CS extract, or a blank control of extract alone. At days 1, 2, and 3 of incubation, the  
331 proliferative capacity of the cells in each group was examined using the MTT method [45].

332 4.3.2. Cell Proliferation Assay of hPDLSCs Loaded on TGF- $\beta$ 3/CS

333 Five different concentrations of TGF- $\beta$ 3 (0, 12, 62.5, 250, and 1000 ng/mL) were loaded on CS.  
334 hPDLSCs were seeded in 24-well plates preloading TGF- $\beta$ 3/CS at a density of  $2 \times 10^4$  cells/well. The  
335 viability of the cells was determined using a CCK-8 assay (Enhanced Cell Counting Kit-8, Beyotime,  
336 Shanghai, China).

337 hPDLSCs were seeded in 96-well plates at a density of  $5 \times 10^3$  cells/well, then treated with  
338 different concentrations of TGF- $\beta$ 3 (0, 12, 62.5, 250, 500, and 1000 ng/mL). Cell proliferation was  
339 evaluated using an MTT assay.

340 A microplate reader (Thermo Lab systems, Waltham, MA, USA) was used to detect the  
341 absorbance at 570nm (MTT assay) or 450 nm (CCK-8 assay) after shaking samples for 5 min. Each  
342 assay was performed in triplicate.

343 4.3.3. Growth of hPDLSCs Implanted in TGF- $\beta$ 3/CS

344 To further study cell growth on TGF- $\beta$ 3/CS, hPDLSCs were cultured on TGF- $\beta$ 3/CS for 3 days  
345 and stained by Calcein AM/PI (Calcein-AM/PI Double Stain Kit, Shanghai, China), followed by  
346 fluorescence microscopy (LSM700, Zeiss, Jena, Germany) to observe the fluorescence degree.

347 hPDLSCs pre-stained with CM-Dil (BestBio, Shanghai, China) were loaded on TGF- $\beta$ 3/CS and  
348 implanted subcutaneously into Sprague-Dawley (SD) rats ( $280 \pm 20$  g, male,  $n = 15$ ; no.  
349 37009200016139) for 7, 14, and 21 days. Animals were sacrificed at 2 and 4 weeks. All the procedures  
350 for mice handling were based on the principles (ref 006939801/2010-00810) of Laboratory Animal Care  
351 formulated by the National Society for Medical Research and approved by the Ethics Review  
352 Committee for Animal Experimentation of Jinan University (ethical review no. 2019346), Guangzhou,  
353 China. Experiments complied with the National Institutes of Health guide for the care and use of  
354 Laboratory animals (NIH Publications No. 8023, revised 1996). Samples were harvested with the  
355 surrounding tissue, followed by examination with fluorescence microscopy (LSM700, Zeiss, Jena,  
356 Germany) to observe the fluorescence degree.

## 357 4.4. Induction of Osteogenic Differentiation

358 hPDLSCs (P3) were seeded into 12-well plates at  $5 \times 10^4$  cells/well and cultured until they  
359 reached 80% confluence. Then, hPDLSCs were cultivated in osteogenic differentiation medium,  
360 containing  $10^{-8}$  M dexamethasone (Sigma-Aldrich, St. Louis, MO, USA), 10 mM  $\beta$ -glycerophosphate  
361 (Sigma-Aldrich, St. Louis, Missouri, USA), and 50 ng/mL ascorbic acid (Sigma-Aldrich, St. Louis, MO,  
362 USA) in  $\alpha$ -MEM with 10% FBS and 1% penicillin-streptomycin. The osteogenic medium was changed  
363 every 2 days.

364 Induction of hPDLSCs was completed with different concentrations of TGF- $\beta$ 3 (0, 62.5, 250, and  
365 500 ng/mL). After cultivation for 3 and 7 days, we stained the hPDLSCs with an Alkaline phosphatase  
366 (ALP) staining kit (Beyotime Institute of Biotechnology, Shanghai, China) to ensure early osteogenic  
367 differentiation capacity. After cultivation for 14 days, we stained the hPDLSCs with alizarin red  
368 (Cyagen Biosciences, CA, USA) to ensure the late osteogenic differentiation capacity of hPDLSCs.

369 Four different concentrations of TGF- $\beta$ 3 (0, 62.5, 250, and 500 ng/mL) were loaded in CS. After  
370 cultivation for 3, 7, and 14 days, we determined the ALP activity of hPDLSCs on TGF- $\beta$ 3/CS using an  
371 ALP staining kit (Beyotime Institute of Biotechnology, Shanghai, China). For the detection and  
372 quantification of osteocalcin in hPDLSCs in the late stage of each group of materials, a calcium  
373 colorimetric assay (Sigma-Aldrich, St. Louis, MO, USA) was used after cultivation for 14, 21, and 28  
374 days.

## 375 4.5. Western Blot Analysis

376 After 7 and 14 days of cultivation, cells were digested and collected. The cell pellets were lysed  
377 in a RIPA buffer (Cell Signaling Technology, Beverly, MA, USA) on ice for 30 mins, and then  
378 centrifuged at 12,000 rpm and 4 °C for 30 min. The supernatants were collected, and the protein  
379 concentrations were measured with a BCA protein assay kit (Life Technologies, Carlsbad, CA, USA)

according to the manufacturer's instructions. Sodium dodecyl sulfate polyacrylamide gel electrophoresis and immunoblot analysis were conducted according to standard protocols and visualized using the ChemiDoc-It Imaging System (UVP, Upland, MA, USA). The TGF- $\beta$ RI, TGF- $\beta$ RII, p38, Pp38, COLI (Affinity Biosciences, OH, USA), ALPL (Alkaline phosphatase), COLII (Abcam, Cambridge, MA, USA), GAPDH antibodies, and their phosphorylated patterns, as well as HRP-conjugated secondary antibody (Cell Signaling Technology, Boston, MA, USA) were used.

#### 4.6. Statistical Analysis

Data are reported as mean  $\pm$  standard deviation. To evaluate the statistical significance of the data, groups were compared in GraphPad Prism 6 (GraphPad Software Inc., La Jolla, CA, USA) by one-way analysis of variance (ANOVA) followed by Tukey's test.  $P$  values  $< 0.05$  were considered statistically significant.

### 5. Conclusions

TGF- $\beta$ 3 had no effect on the proliferation of hPDLSCs, but an appropriate concentration of TGF- $\beta$ 3 could promote the osteogenic differentiation of hPDLSCs via activation of the p38 MAPK pathway. The prepared TGF- $\beta$ 3/CS has a good water absorption rate, swelling ratio, and porosity; is favorable for the adhesion, spreading and growth of seed cells; has good biosafety; and conforms to the medical standard of biological materials. TGF- $\beta$ 3/CS can promote the osteogenic differentiation of hPDLSCs, and the combination of the two is expected to be used for the repair of alveolar bone defects.

**Acknowledgments:** This work was supported by the Major Scientific and Technological Special Project of the Administration of Ocean and Fisheries of Guangdong Province (GDME-2018C013, Yuecainong, 2017, no.17), Guangzhou Science and Technology Program key projects (201803010044) and Science and technology program of Tianhe District, Guangzhou City (201704YG066).

**Conflicts of Interest:** The authors declare no conflicts of interest.

### References

1. Goker, F.; Larsson, L.; Del Fabbro, M.; Asa'ad, F. Gene delivery therapeutics in the treatment of periodontitis and peri-implantitis: A state of the art review. *Int J Mol Sci* **2019**, *20*.
2. Shanbhag, S.; Pandis, N.; Mustafa, K.; Nyengaard, J.R.; Stavropoulos, A. Alveolar bone tissue engineering in critical-size defects of experimental animal models: A systematic review and meta-analysis. *Journal of tissue engineering and regenerative medicine* **2017**, *11*, 2935-2949.
3. Larsson, L.; Decker, A.M.; Nibali, L.; Pilipchuk, S.P.; Berglundh, T.; Giannobile, W.V. Regenerative medicine for periodontal and peri-implant diseases. *Journal of dental research* **2016**, *95*, 255-266.
4. Al-Askar, M.; Alsaffar, D. Feasibility of using allograft bone with resorbable collagen membrane for alveolar ridge vertical defect augmentation for dental implant placement in patient with aggressive periodontitis: A case report. *Saudi Dent J* **2018**, *30*, 256-259.
5. Akintoye, S.O. The distinctive jaw and alveolar bone regeneration. *Oral Dis* **2018**, *24*, 49-51.
6. EzEldeen, M.; Wyatt, J.; Al-Rimawi, A.; Coucke, W.; Shaheen, E.; Lambrechts, I.; Willems, G.; Politis, C.; Jacobs, R. Use of cbct guidance for tooth autotransplantation in children. *Journal of dental research* **2019**, *98*, 406-413.
7. Gjerde, C.; Mustafa, K.; Helle, S.; Rojewski, M.; Gjengedal, H.; Yassin, M.A.; Feng, X.; Skaale, S.; Berge, T.; Rosen, A., et al. Cell therapy induced regeneration of severely atrophied mandibular bone in a clinical trial. *Stem cell research & therapy* **2018**, *9*, 213.
8. Kloss, F.R.; Offermanns, V.; Kloss-Brandstatter, A. Cecomparison of allogeneic and autogenous bone grafts for augmentation of alveolar ridge defects-a 12-month retrospective radiographic evaluation. *Clin Oral Implants Res* **2018**.
9. Hameed, M.H.; Gul, M.; Ghafoor, R.; Khan, F.R. Vertical ridge gain with various bone augmentation techniques: A systematic review and meta-analysis. *J Prosthodont* **2019**.
10. Ivgilia, G.; Kargozar, S.; Baino, F. Biomaterials, current strategies, and novel nano-technological approaches for periodontal regeneration. *Journal of functional biomaterials* **2019**, *10*.
11. Urban, I.A.S.; Montero, E.; Monje, A.; Sanz-Sanchez, I. Effectiveness of vertical ridge augmentation interventions. A systematic review and meta-analysis. *J Clin Periodontol* **2019**.

430 12. Reynolds, M.A.; Kao, R.T.; Camargo, P.M.; Caton, J.G.; Clem, D.S.; Fiorellini, J.P.; Geisinger, M.L.; Mills, M.P.; Nares, S.; Nevins, M.L. Periodontal regeneration - intrabony defects: A consensus report from the aap regeneration workshop. *Journal of periodontology* **2015**, *86*, S105-107.

431 13. Bottino, M.C.; Thomas, V.; Schmidt, G.; Vohra, Y.K.; Chu, T.M.; Kowolik, M.J.; Janowski, G.M. Recent 432 advances in the development of gtr/gbr membranes for periodontal regeneration--a materials perspective. 433 *Dental materials : official publication of the Academy of Dental Materials* **2012**, *28*, 703-721.

434 14. Rakhmatia, Y.D.; Ayukawa, Y.; Furuhashi, A.; Koyano, K. Current barrier membranes: Titanium mesh and 435 other membranes for guided bone regeneration in dental applications. *J Prosthodont Res* **2013**, *57*, 3-14.

436 15. Soldatos, N.K.; Stylianou, P.; Koidou, V.P.; Angelov, N.; Yukna, R.; Romanos, G.E. Limitations and options 437 using resorbable versus nonresorbable membranes for successful guided bone regeneration. *Quintessence Int* **2017**, *48*, 131-147.

438 16. Sasaki, H.; Rothrauff, B.B.; Alexander, P.G.; Lin, H.; Gottardi, R.; Fu, F.H.; Tuan, R.S. In vitro repair of 439 meniscal radial tear with hydrogels seeded with adipose stem cells and tgf-beta3. *The American journal of 440 sports medicine* **2018**, *46*, 2402-2413.

441 17. Lee, H.L.; Yu, B.; Deng, P.; Wang, C.Y.; Hong, C. Transforming growth factor-beta-induced kdm4b 442 promotes chondrogenic differentiation of human mesenchymal stem cells. *Stem Cells* **2016**, *34*, 711-719.

443 18. Yang, Q.; Teng, B.H.; Wang, L.N.; Li, K.; Xu, C.; Ma, X.L.; Zhang, Y.; Kong, D.L.; Wang, L.Y.; Zhao, Y.H. Silk 444 fibroin/cartilage extracellular matrix scaffolds with sequential delivery of tgf-beta3 for chondrogenic 445 differentiation of adipose-derived stem cells. *International journal of nanomedicine* **2017**, *12*, 6721-6733.

446 19. Jing, H.; Zhang, X.; Gao, M.; Luo, K.; Fu, W.; Yin, M.; Wang, W.; Zhu, Z.; Zheng, J.; He, X. Kartogenin 447 preconditioning commits mesenchymal stem cells to a precartilaginous stage with enhanced chondrogenic 448 potential by modulating jnk and beta-catenin-related pathways. *FASEB journal : official publication of the 449 Federation of American Societies for Experimental Biology* **2019**, fj201802137RRR.

450 20. Grafe, I.; Alexander, S.; Peterson, J.R.; Snider, T.N.; Levi, B.; Lee, B.; Mishina, Y. Tgf-beta family signaling 451 in mesenchymal differentiation. *Cold Spring Harbor perspectives in biology* **2018**, *10*.

452 21. Deng, M.; Mei, T.; Hou, T.; Luo, K.; Luo, F.; Yang, A.; Yu, B.; Pang, H.; Dong, S.; Xu, J. Tgfbeta3 recruits 453 endogenous mesenchymal stem cells to initiate bone regeneration. *Stem cell research & therapy* **2017**, *8*, 258.

454 22. Ripamonti, U.; Dix-Peek, T.; Parak, R.; Milner, B.; Duarte, R. Profiling bone morphogenetic proteins and 455 transforming growth factor-betas by htgf-beta3 pre-treated coral-derived macroporous bioreactors: The 456 power of one. *Biomaterials* **2015**, *49*, 90-102.

457 23. Ripamonti, U. Developmental pathways of periodontal tissue regeneration: Developmental diversities of 458 tooth morphogenesis do also map capacity of periodontal tissue regeneration? *Journal of periodontal research* 459 **2019**, *54*, 10-26.

460 24. Klar, R.M.; Duarte, R.; Dix-Peek, T.; Ripamonti, U. The induction of bone formation by the recombinant 461 human transforming growth factor-beta3. *Biomaterials* **2014**, *35*, 2773-2788.

462 25. Ripamonti, U.; Ramoshebi, L.N.; Teare, J.; Renton, L.; Ferretti, C. The induction of endochondral bone 463 formation by transforming growth factor-?3: Experimental studies in the non-human primate papio 464 ursinus. *Journal of cellular and molecular medicine* **2007**, *ja*.

465 26. Ripamonti, U.; Duarte, R.; Ferretti, C. Re-evaluating the induction of bone formation in primates. 466 *Biomaterials* **2014**, *35*, 9407-9422.

467 27. Moioli, E.K.; Clark, P.A.; Sumner, D.R.; Mao, J.J. Autologous stem cell regeneration in craniosynostosis. 468 *Bone* **2008**, *42*, 332-340.

469 28. Gupta, A.; Rattan, V.; Rai, S. Efficacy of chitosan in promoting wound healing in extraction socket: A 470 prospective study. *J Oral Biol Craniofac Res* **2019**, *9*, 91-95.

471 29. Safari, S.; Mahdian, A.; Motamedian, S.R. Applications of stem cells in orthodontics and dentofacial 472 orthopedics: Current trends and future perspectives. *World J Stem Cells* **2018**, *10*, 66-77.

473 30. Abdel Meguid, E.; Ke, Y.; Ji, J.; El-Hashash, A.H.K. Stem cells applications in bone and tooth repair and 474 regeneration: New insights, tools, and hopes. *Journal of cellular physiology* **2018**, *233*, 1825-1835.

475 31. Kim, S.H.; Kim, K.H.; Seo, B.M.; Koo, K.T.; Kim, T.I.; Seol, Y.J.; Ku, Y.; Rhyu, I.C.; Chung, C.P.; Lee, Y.M. 476 Alveolar bone regeneration by transplantation of periodontal ligament stem cells and bone marrow stem 477 cells in a canine peri-implant defect model: A pilot study. *Journal of periodontology* **2009**, *80*, 1815-1823.

478 32. Ge, B.; Liu, H.; Liang, Q.; Shang, L.; Wang, T.; Ge, S. Oxytocin facilitates the proliferation, migration and 479 osteogenic differentiation of human periodontal stem cells in vitro. *Arch Oral Biol* **2019**, *99*, 126-133.

480 481 482

483 33. Zhu, Y.; Li, Q.; Zhou, Y.; Li, W. Tlr activation inhibits the osteogenic potential of human periodontal  
484 ligament stem cells through akt signaling in a myd88- or trif-dependent manner. *Journal of periodontology*  
485 **2018**.

486 34. Wang, L.; Wu, F.; Song, Y.; Duan, Y.; Jin, Z. Erythropoietin induces the osteogenesis of periodontal  
487 mesenchymal stem cells from healthy and periodontitis sources via activation of the p38 mapk pathway.  
488 *International journal of molecular medicine* **2018**, *41*, 829-835.

489 35. Chen, G.; Deng, C.; Li, Y.P. Tgf-beta and bmp signaling in osteoblast differentiation and bone formation.  
490 *Int J Biol Sci* **2012**, *8*, 272-288.

491 36. Feldman, D.S.; McCauley, J.F. Mesenchymal stem cells and transforming growth factor-beta(3) (tgf-beta(3))  
492 to enhance the regenerative ability of an albumin scaffold in full thickness wound healing. *Journal of*  
493 *functional biomaterials* **2018**, *9*.

494 37. Menon, A.H.; Soundarya, S.P.; Sanjay, V.; Chandran, S.V.; Balagangadharan, K.; Selvamurugan, N.  
495 Sustained release of chrysin from chitosan-based scaffolds promotes mesenchymal stem cell proliferation  
496 and osteoblast differentiation. *Carbohydrate polymers* **2018**, *195*, 356-367.

497 38. Yu, W.; Jiang, D.; Yu, S.; Fu, J.; Li, Z.; Wu, Y.; Wang, Y. Sall4 promotes osteoblast differentiation by  
498 deactivating notch2 signaling. *Biomedicine & pharmacotherapy = Biomedecine & pharmacotherapie* **2018**, *98*, 9-  
499 17.

500 39. Lin, C.Y.; Chang, Y.H.; Li, K.C.; Lu, C.H.; Sung, L.Y.; Yeh, C.L.; Lin, K.J.; Huang, S.F.; Yen, T.C.; Hu, Y.C.  
501 The use of ascs engineered to express bmp2 or tgf-beta3 within scaffold constructs to promote calvarial  
502 bone repair. *Biomaterials* **2013**, *34*, 9401-9412.

503 40. McDermott, A.M.; Herberg, S.; Mason, D.E.; Collins, J.M.; Pearson, H.B.; Dawahare, J.H.; Tang, R.; Patwa,  
504 A.N.; Grinstaff, M.W.; Kelly, D.J., et al. Recapitulating bone development through engineered mesenchymal  
505 condensations and mechanical cues for tissue regeneration. *Science translational medicine* **2019**, *11*.

506 41. Aisenbrey, E.A.; Bryant, S.J. The role of chondroitin sulfate in regulating hypertrophy during msc  
507 chondrogenesis in a cartilage mimetic hydrogel under dynamic loading. *Biomaterials* **2019**, *190-191*, 51-62.

508 42. Guerrero, J.; Pigeot, S.; Muller, J.; Schaefer, D.J.; Martin, I.; Scherberich, A. Fractionated human adipose  
509 tissue as a native biomaterial for the generation of a bone organ by endochondral ossification. *Acta*  
510 *biomaterialia* **2018**, *77*, 142-154.

511 43. Paolella, F.; Gabusi, E.; Manferdini, C.; Schiavonato, A.; Lisignoli, G. Specific concentration of hyaluronan  
512 amide derivative induces osteogenic mineralization of human mesenchymal stromal cells: Evidence of  
513 runx2 and col1a1 genes modulation. *Journal of biomedical materials research. Part A* **2019**.

514 44. Douglas, T.E.L.; Vandrovova, M.; Krocilova, N.; Keppler, J.K.; Zarubova, J.; Skirtach, A.G.; Bacakova, L.  
515 Application of whey protein isolate in bone regeneration: Effects on growth and osteogenic differentiation  
516 of bone-forming cells. *J Dairy Sci* **2018**, *101*, 28-36.

517 45. Zang, S.; Dong, G.; Peng, B.; Xu, J.; Ma, Z.; Wang, X.; Liu, L.; Wang, Q. A comparison of physicochemical  
518 properties of sterilized chitosan hydrogel and its applicability in a canine model of periodontal  
519 regeneration. *Carbohydrate polymers* **2014**, *113*, 240-248.

520 46. Yoshio, S.; Hiroaki, T.; Masahide, T.; Kenichiro, M.; Tomomi, N.; Keigo, S.; Mariko, K.; Toshihito, A.;  
521 Hiroyuki, O.; Takanobu, K. Fibroblast growth factor-2 stimulates directed migration of periodontal  
522 ligament cells via pi3k/akt signaling and cd44/hyaluronan interaction. *Journal of Cellular Physiology* **2011**,  
523 *226*, 809-821.